

Supplementary Materials for

Structural insights into the EGO-TC-mediated membrane tethering of the TORC1-regulatory Rag GTPases

Tianlong Zhang, Marie-Pierre Péli-Gulli, Zhen Zhang, Xin Tang, Jie Ye, Claudio De Virgilio*, Jianping Ding*

*Corresponding author. Email: claudio.devirgilio@unifr.ch (C.D.V.); jpding@sibcb.ac.cn (J.D.)

Published 25 September 2019, *Sci. Adv.* **5**, eaax8164 (2019)

DOI: 10.1126/sciadv.aax8164

This PDF file includes:

- Fig. S1. Sequence alignment of Ego1 from different species as analyzed by ESPript 3.0 (34).
- Fig. S2. Deletion of residues 98 to 121 of Ego1 does not affect the vacuolar membrane location of Ego1 nor the subsequent vacuolar recruitment of the other EGO components.
- Fig. S3. Strains expressing Ego1 and Ego3 mutant variants that are unable to bind the Rag GTPases are sensitive to rapamycin and have reduced TORC1 activity.
- Fig. S4. Overall structure of the two EGO molecules in the asymmetric unit.
- Fig. S5. Representative composite 2Fo-Fc omit maps (contoured at 1σ) of the EGO (molecule A).
- Fig. S6. Structural comparison of associated and free Gtr1-Gtr2 heterodimers.
- Fig. S7. Structural comparison of the EGO and the Ragulator-Rag complex.
- Fig. S8. Analysis of the diffraction data with the Diffraction Anisotropy Server (26).
- Table S1. Strains used in this study.
- Table S2. Plasmids used in this study.
- References (34–38)

Supplementary Materials

Supplementary Figures

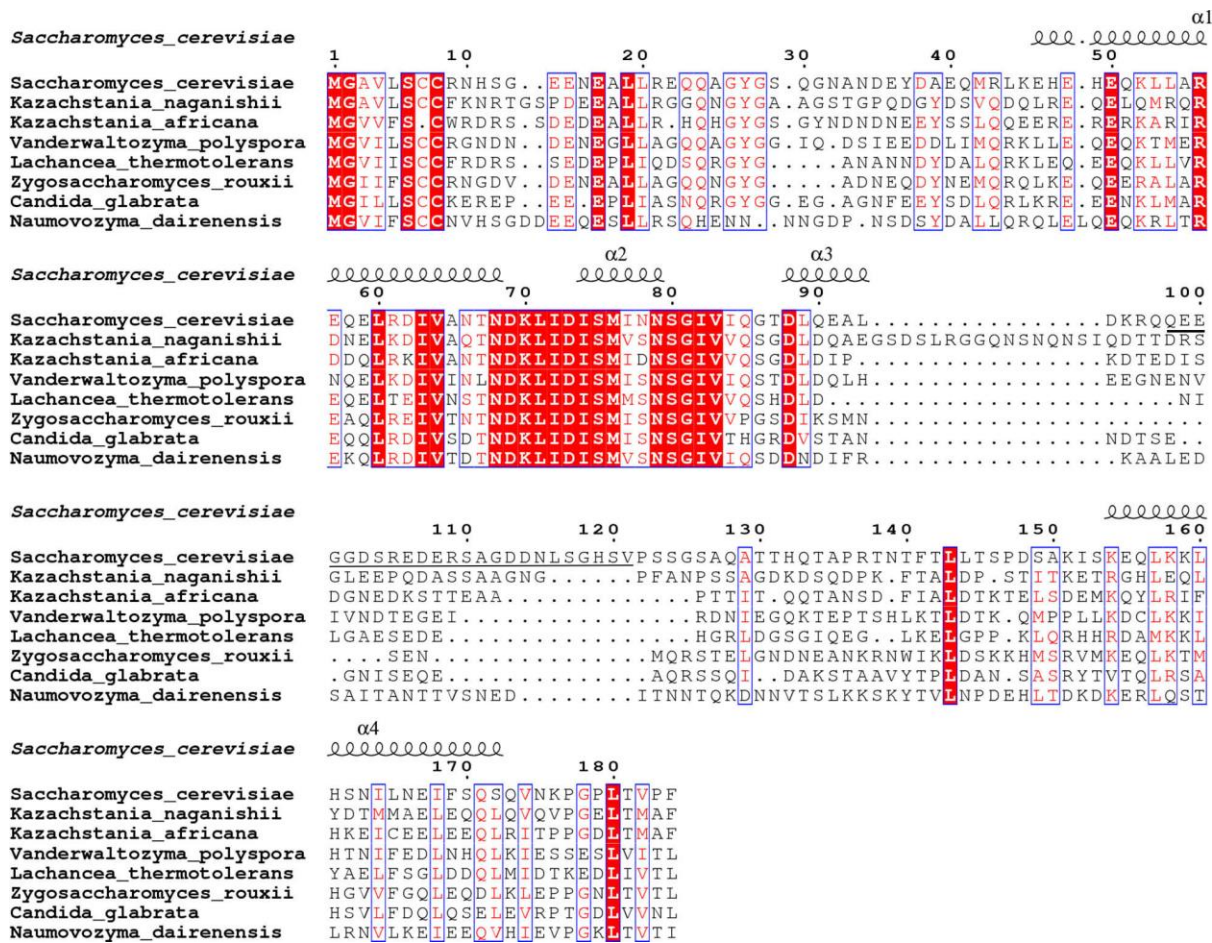


Fig. S1. Sequence alignment of Ego1 from different species as analyzed by ESPrict 3.0 (34). The secondary structures ($\alpha 1$ - $\alpha 4$) of Ego1 in the EGOE are schematized above the alignment. Residues 98-121 of *Saccharomyces cerevisiae* Ego1 which were deleted in the construct are underlined.

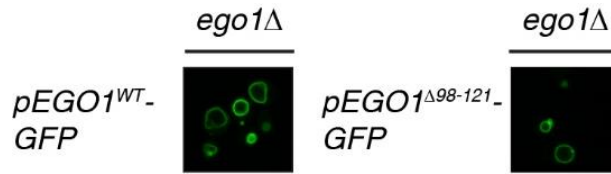
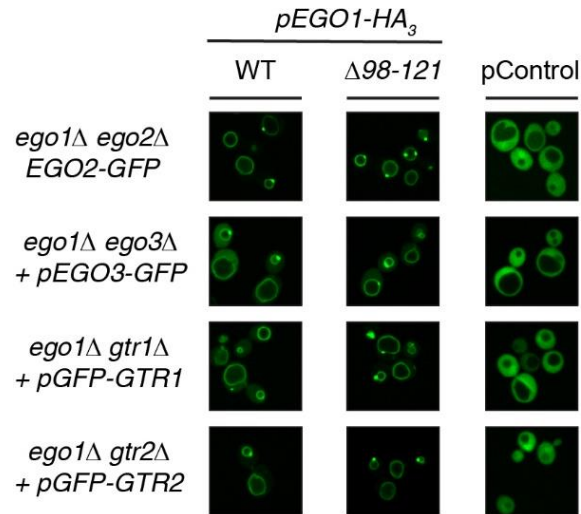
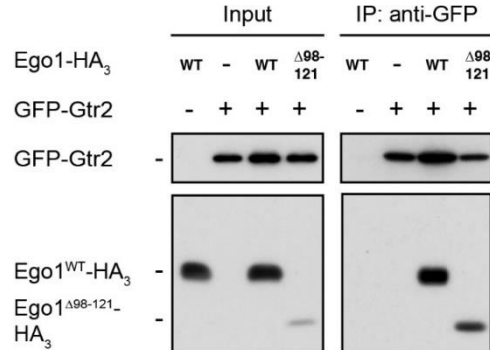
A**B****C**

Fig. S2. Deletion of residues 98 to 121 of Ego1 does not affect the vacuolar membrane location of Ego1 nor the subsequent vacuolar recruitment of the other EGO components. (A) Ego1^{Δ98-121}-GFP readily localizes to the vacuolar limiting membrane. Localization of plasmid-expressed Ego1^{WT}-GFP or Ego1^{Δ98-121}-GFP was examined in prototrophic *ego1Δ* cells grown exponentially in synthetic drop out medium. (B) The EGO components are efficiently recruited to the vacuolar rim by Ego1^{Δ98-121}-HA₃. Localization of each plasmid-expressed GFP-tagged EGO component was determined in indicated prototrophic strains co-expressing, or not (pControl), Ego1^{WT}-HA₃ or Ego1^{Δ98-121}-HA₃, and cultured as in A. (C) Ego1^{Δ98-121} and Gtr2 interact with each other. Anti-GFP immunoprecipitations were performed on lysates from a subset of cells described in panel (B; bottom row) or from *ego1Δ* cells expressing Ego1^{WT}-HA₃. Input and IP fractions were analyzed by western blot and probed with anti-HA and anti-GFP antibodies.

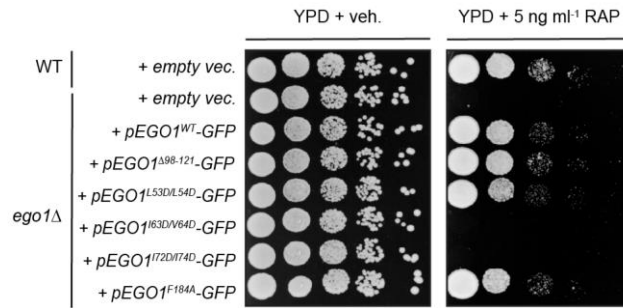
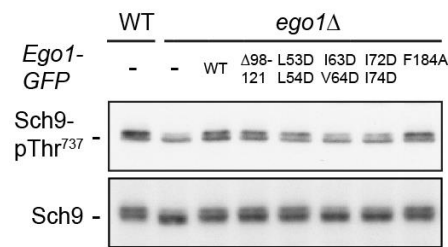
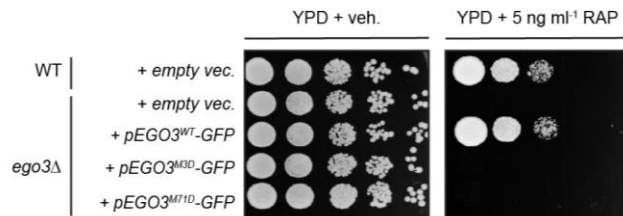
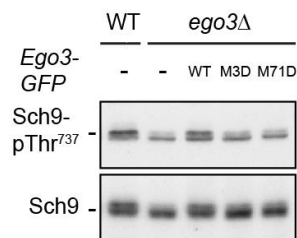
A**B****C****D**

Fig. S3. Strains expressing Ego1 and Ego3 mutant variants that are unable to bind the Rag GTPases are sensitive to rapamycin and have reduced TORC1 activity. (A-B) Prototrophic *WT* and *ego1Δ* strains expressing, or not (+ empty vec; -), the indicated plasmid-expressed Ego1-GFP variants were grown exponentially in synthetic defined dropout medium. Serial 10-fold dilutions were then spotted on YPD plates supplemented with vehicle (veh.) or 5 ng ml⁻¹ rapamycin (RAP) and incubated for 4 days at 30°C (A). Alternatively, *in vivo* TORC1 activity was assessed by examining the phosphorylation status of Thr⁷³⁷ within the TORC1 target Sch9 by immunoblot analysis using anti-Sch9-pThr⁷³⁷ and anti-Sch9 antibodies (B). **(C-D)** Prototrophic *WT* and *ego3Δ* strains expressing, or not (+ empty vec; -), the indicated

plasmid-expressed Ego3-GFP variants were grown and treated as in (A) and (B), respectively.

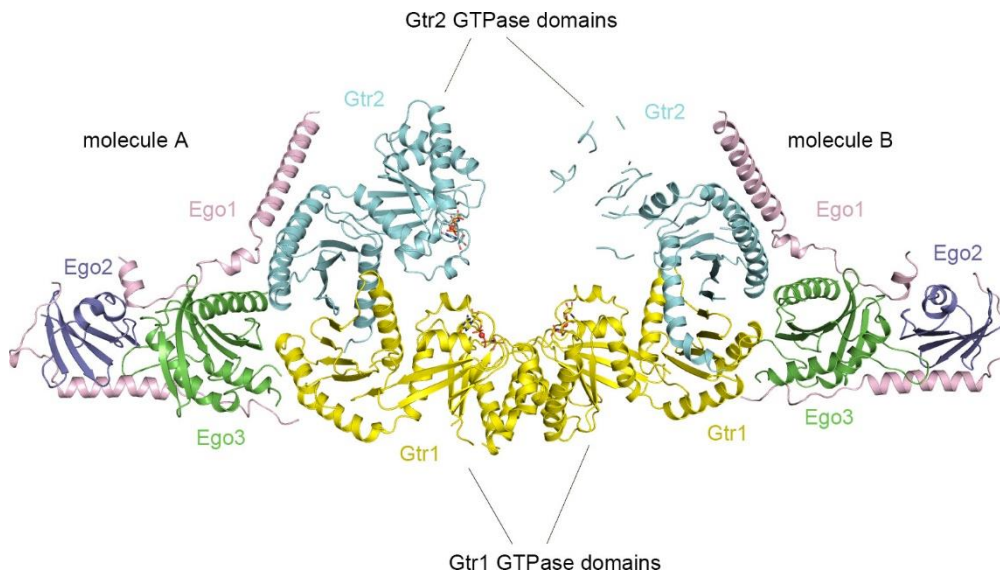
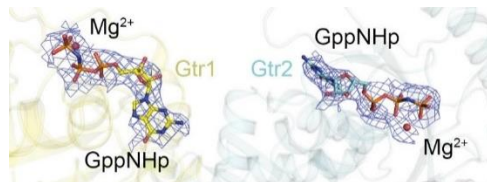
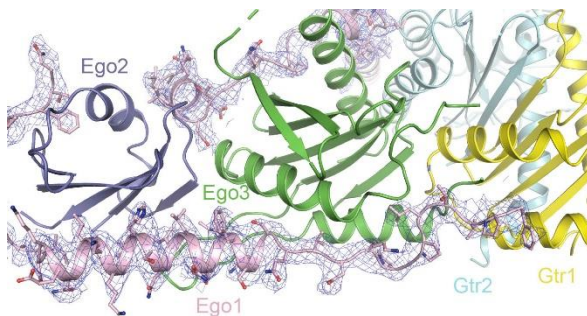


Fig. S4. Overall structure of the two EGOC molecules in the asymmetric unit. The color codes of the components are the same as in Fig. 1B.

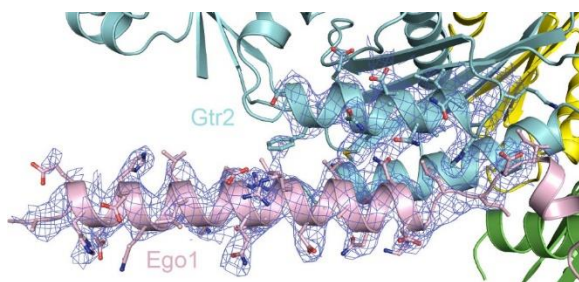
A



B



C



D

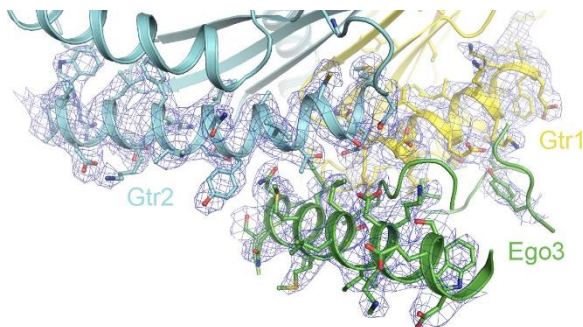


Fig. S5. Representative composite 2Fo-Fc omit maps (contoured at 1σ) of the EGOc (molecule A).

(A) The bound GppNHp molecules and Mg²⁺ ions in Gtr1-Gtr2. The color codes of the components are the same as in Fig. 1B. (B) Ego1 in the interaction interfaces with Ego2, Ego3, and Gtr1. (C) The interaction interface between the α1-helix of Ego1 and Gtr2. (D) The interaction interface between Ego3 and Gtr1-Gtr2.

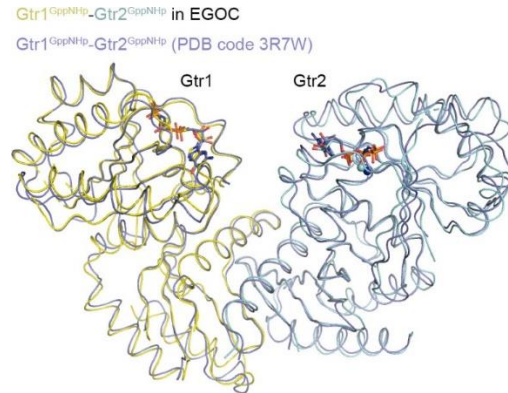
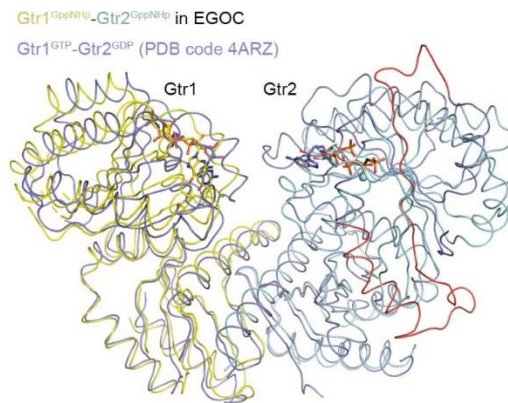
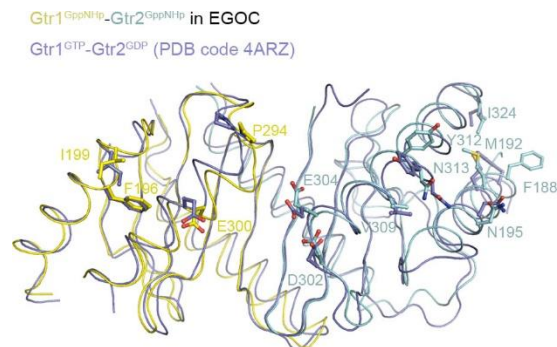
A**B****C**

Fig. S6. Structural comparison of associated and free Gtr1-Gtr2 heterodimers. (A) Superposition of the structures of Gtr1^{GppNHp}-Gtr2^{GppNHp} in the EGOc (colored as in Fig. 1B) and free Gtr1^{GppNHp}-Gtr2^{GppNHp} (PDB code 3R7W) (colored in blue). (B) Superposition of the structures of Gtr1^{GppNHp}-Gtr2^{GppNHp} in the EGOc and free Gtr1^{GTP}-Gtr2^{GDP} (PDB code 4ARZ) (colored in blue). The segment composed of residues 28-70 of Gtr2^{GDP}, which exhibits a conformational rearrangement, is colored in red. (C) Superposition of the Roadblock domains of Gtr1^{GppNHp}-Gtr2^{GppNHp} in the EGOc and free Gtr1^{GTP}-Gtr2^{GDP} (PDB code 4ARZ) (colored in blue). The residues involved in the interactions with Ego1 and Ego3 are shown in ball-and-stick models.

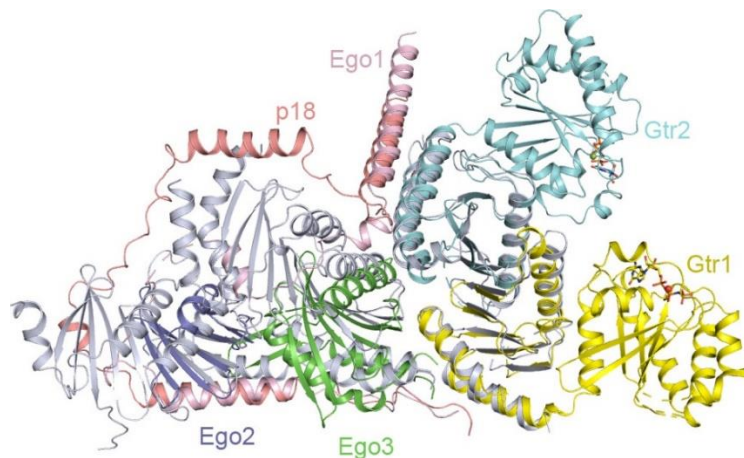
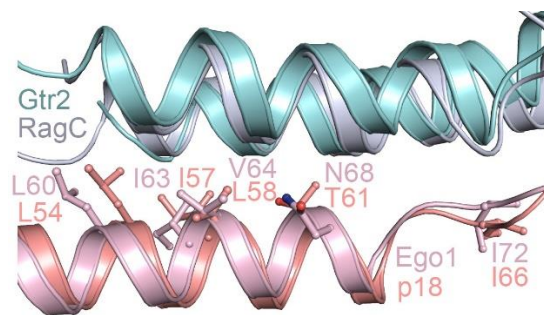
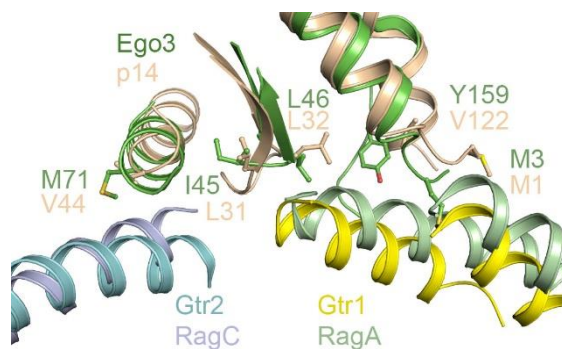
A**B****C**

Fig. S7. Structural comparison of the EGO and the Regulator-Rag complex. (A) The Regulator-RagA(CTD)-RagC(CTD) complex (PDB code 6EHR) is superimposed onto the EGO. The color codes of the EGO components are the same as in Fig. 1B. For clarity, p18 is colored in red and the other components in the Regulator-Rag complex are colored in gray. (B) Comparison of the residues from the α 1-helix of Ego1 and p18 in the interacting interfaces with Gtr2/RagC. Ego1, p18, Gtr2, and RagC are colored in pink, red, cyan, and gray, respectively. (C) Comparison of the residues from Ego3 and p14 in the interaction interfaces with Gtr1/RagA and Gtr2/RagC. Ego3, p14, Gtr1, Gtr2, RagA, and RagC are colored in green, wheat, yellow, cyan, palegreen, and gray, respectively.

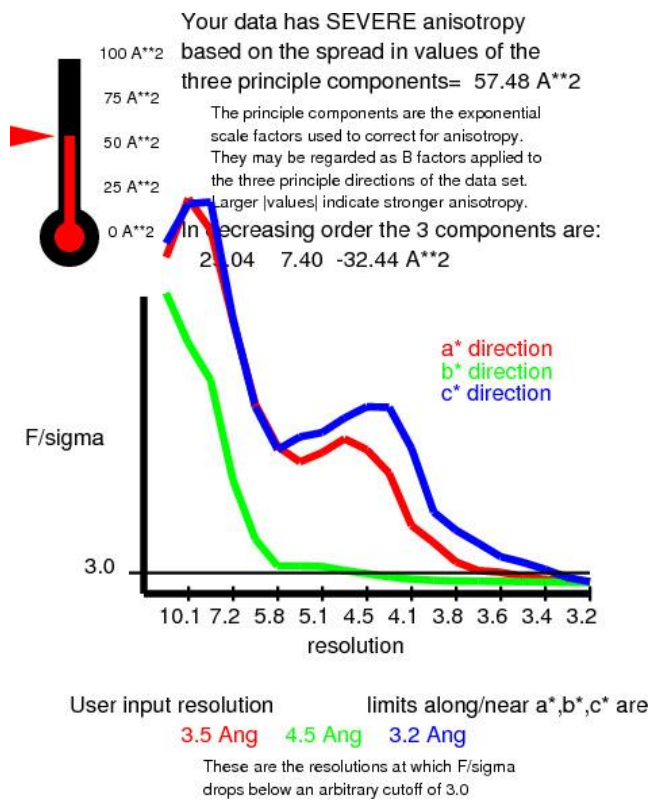


Fig. S8. Analysis of the diffraction data with the Diffraction Anisotropy Server (26). Based on the analysis of the server, the anisotropic native dataset for the EGOc is truncated to 3.5, 4.5 and 3.2 Å resolution along the reciprocal space directions a*, b* and c*, respectively. The figure was generated with the server.

Supplementary Tables

Table S1. Strains used in this study.

Strain	Genotype	Source	Figure
KT1960	<i>MATα; his3, leu2, ura3-52, trp1</i>	(35)	
KT1961	<i>MATα; his3, leu2, ura3-52, trp1</i>	(35)	S3A-D
MP2649	[KT1960] <i>ego1Δ::KanMX4</i>	This study	3A, C, E; S2A, C; S3A, B
MP279-18A	[KT1961] <i>ego1Δ::KanMX4, gtr2Δ::NatMX4</i>	(18)	3B, C; S2B, C
MP279-18B	[KT1960] <i>ego1Δ::KanMX4, gtr1Δ::NatMX4</i>	(18)	3D, E; S2B
MP2650	[KT1961] <i>ego3Δ::KanMX4</i>	(21)	3F, H; S3C, D
MP5811	[KT1961] <i>ego3Δ::KanMX4, gtr1Δ::NatMX4, URA3::GTR1p-GFP-GTR1</i>	This study	3G, H
MP5854	[KT1961] <i>ego1Δ::NatMX4, ego2Δ::KanMX6, HIS3::EGO2p-EGO2-GFP</i>	This study	S2B
MP278-1A	[KT1960] <i>ego1Δ::KanMX4, ego3Δ::KanMX4</i>	This study	S2B

Table S2. Plasmids used in this study.

Plasmid	Genotype	Source	Figure
pRS413	CEN, ARS, <i>HIS3</i>	(36)	3A-E, G, H; S2A-C; S3A-D
pRS414	CEN, ARS, <i>TRP1</i>	(36)	3A-H; S2A-C; S3A-D
pRS415	CEN, ARS, <i>LEU2</i>	(36)	3A, C, E-H; S2A-C; S3A-D
pRS416	CEN, ARS, <i>URA3</i>	(36)	3B-H; S2B, C; S3A-D
YCplac33	CEN, ARS, <i>URA3</i>	(37)	
pMP3726	[YCplac33] <i>EGO1p-EGO1^{WT}-(GA)₅-GFP</i>	This study	3A; S2A; S3A, B
pMP3727	[YCplac33] <i>EGO1p-EGO1^{A98-121}-(GA)₅-GFP</i>	This study	S2A; S3A, B
pMP3728	[YCplac33] <i>EGO1p-EGO1^{L53DL54D}-(GA)₅-GFP</i>	This study	3A; S3A, B
pMP3729	[YCplac33] <i>EGO1p-EGO1^{I63DV64D}-(GA)₅-GFP</i>	This study	3A; S3A, B
pMP3737	[YCplac33] <i>EGO1p-EGO1^{I72DI74D}-(GA)₅-GFP</i>	This study	3A; S3A, B
pMP3749	[YCplac33] <i>EGO1p-EGO1^{F184A}-(GA)₅-GFP</i>	This study	3A; S3A, B
pRH2836	[pRS415] <i>GTR2p-GFP-GTR2</i>	Lab stock	3B, C; S2B, C
pMP2736	[YCplac33] <i>EGO1p-EGO1^{WT}-HA₃</i>	This study	3B-E; S2B, C
pMP3730	[YCplac33] <i>EGO1p-EGO1^{L53DL54D}-HA₃</i>	This study	3B, C
pMP3738	[YCplac33] <i>EGO1p-EGO1^{A98-121}-HA₃</i>	This study	S2B, C
pMP3739	[YCplac33] <i>EGO1p-EGO1^{I63DV64D}-HA₃</i>	This study	3B, C
pMP3740	[YCplac33] <i>EGO1p-EGO1^{I72DI74D}-HA₃</i>	This study	3B, C
pMP3750	[YCplac33] <i>EGO1p-EGO1^{F184A}-HA₃</i>	This study	3D, E
pRH2835	[pRS415] <i>GTR1p-GFP-GTR1</i>	Lab stock	3D, E; S2B
pMP2180	[pRS413] <i>EGO3p-EGO3^{WT}-GFP</i>	(38)	3F; S2B; S3C, D
pMP3751	[pRS413] <i>EGO3p-EGO3^{M3D}-GFP</i>	This study	3F; S3C, D
pMP3753	[pRS413] <i>EGO3p-EGO3^{M71D}-GFP</i>	This study	3F; S3C, D
pMP3710	[pRS413] <i>EGO3p-EGO3^{WT}-HA₃</i>	This study	3G, H
pMP3754	[pRS413] <i>EGO3p-EGO3^{M3D}-HA₃</i>	This study	3G, H
pMP3756	[pRS413] <i>EGO3p-EGO3^{M71D}-HA₃</i>	This study	3G, H

pSIVu	integrative, <i>URA3</i>	(38)	
pMP3439	[pSIVu] <i>GTR1p-GFP-GTR1</i>	This study	3G, H
pSIVh	integrative, <i>HIS3</i>	(38)	
pLD3696	[pSIVh] <i>EGO2p-EGO2-GFP</i>	Lab stock	S2B
